

**"A Cochlear Nucleus Auditory
prosthesis based on microstimulation"**

Contract No. **No. NO1-DC-4-0005**
Progress Report #3

HUNTINGTON MEDICAL RESEARCH INSTITUTES
NEURAL ENGINEERING LABORATORY
734 Fairmount Avenue
Pasadena, California 91105

D.B. McCreery, Ph.D.
L.A. Bullara, B.S.
Martin Han, Ph.D.
A.S. Lossinsky, Ph.D.

HOUSE EAR INSTITUTE
2100 WEST THIRD STREET
Los Angeles, California 90057

R.V. Shannon Ph.D
S. Otto M.S.
M. Waring, Ph.D

Summary and abstract

Results from the patients implanted with the penetrating microstimulating array.

All 5 recipients of the penetrating microstimulating array are able to use their implants with varying benefit.. Two patients did not receive hearing on their penetrating electrodes, but all patients' surface electrodes have provided auditory sensations. The penetrating (PABI) array provides hearing sensations at lower levels of electrical stimulation than the surface ABI, with a range of pitch sensations, and with objective and subjective benefits when used in combination with surface electrodes.

Changes to the human penetrating auditory brainstem implant (PABI) array

In two of our patients with the penetrating auditory brainstem implants the stimulus amplitude has been limited by the charge limit of 3 nC/phase, rather than by the patients' judgement of maximum comfortable loudness. Therefore, it might be advantageous to raise the charge limits somewhat, if this can be done without injury to the neurons and neuropil surrounding the electrodes. We propose to increase the microelectrodes' exposed surface areas, thereby reducing the charge density and current density in the tissue immediately adjacent to the electrode. We investigated this approach in two domestic cats. In the first (CN150), the safety of stimulating at higher charge per phase and lower charge density was investigated, In the second cat (CN151), we investigated how the larger electrode surface area might affect the neuronal activity induced by the microstimulation at levels near the threshold of the auditory percepts in the human patients. In one cat (CN150), we investigated the histologic affects of stimulating continuously for 7 hours at 6 or 8 nC/ph at a pulse rate of 250 Hz. The stimulation was conducted 37 days after implanting the microelectrode array into the cochlear nucleus. Histologic evaluation of the electrode sites showed no differences between the pulsed and unpulsed electrode sites, except for some minimal infiltration of inflammatory cells near the pulse sites which is always seen around pulsed microelectrodes.

In another animal (cat CN151), we conducted an acute experiment to determine how the responses evoked in the feline cochlear nucleus might differ when the electrode surface area is increased to 5,000 μm^2 from the present 2,000 μm^2 . In the human patients, the threshold of auditory percepts evoked from the penetrating microelectrodes has been in the range of 0.5-1.0 nC/ph. In cat CN151, two microelectrode, one of each 2 size, were inserted into the cochlear nucleus, and the compound evoked response was recorded in the contralateral inferior colliculus. There were no consistent differences in the neuronal response evoked by the 2 sizes of microelectrodes. This implies that the threshold of the patient's auditory percepts would not be influenced significantly if the surface area of the microelectrodes is increased to 5,000 μm^2 from the present 2,000 μm^2 .

We also are proposing to convert the 2 stabilizing pins to active electrodes, by opening an annular "window" on the side of each, 2.5 mm below the array button (superstructure).

Evaluation of chronically-implanted silicon-substrate microelectrode arrays In the cat cochlear nucleus

We are developing arrays of silicon substrate microelectrodes which will allow placement of many more electrode sites into the human cochlear nucleus than is possible with arrays of discrete microelectrodes. We have been implanting these arrays chronically into the ventral cochlear nucleus of cats. Over the course of 237 days, the response growth functions (RGFs) of the compound response recorded in the inferior colliculus shows good stability when evoked from microelectrode sites between 1.2 and 1.9 mm beneath the surface of the CN, but showed marked diminution when evoked from sites approximately 0.8 mm below the dorsolateral

surface of the cochlear nucleus. This could be due to the growth of connective tissue under the array superstructure which would, in effect, move the electrode sites to positions that are more dorsal in the nucleus. In subsequent cats, we have used arrays with a new probe design in which the electrode sites are slightly farther from the probe's spine, and thus, will be slightly deeper in the cochlear nucleus. Preliminary results from 2 of these animals (CN152 & CN153) are described.

I/ Activities at the House Ear Institute related to the intranuclear microstimulating array (“Penetrating auditory brainstem implant, PABI)

Patients seen in follow-up:

All five PABI patients were seen in the first quarter of 2005. Routine clinical follow-up includes measurement of thresholds and MCL levels on each electrode, rechecking electrodes that previously produced non-auditory side effects, and adjusting the mappings on the three speech processors given each patients: surface-only map, penetrating-only map (if possible), and combination surface-penetrating map. Psychophysical testing was performed if the patient's health and schedule allow. More detailed reports of the clinical and psychophysical data and analysis will be presented in future progress reports of this contract. In the first quarter of 2005 patient contacts were:

Jan 11 and 12. PABI #3 (9 mos follow-up). Electrical threshold and MCL levels stable. Side effects were unchanged. PABI #3 used the device infrequently due to normal residual hearing in non-PABI ear. Psychophysical tests focused on modulation detection as a function of modulation frequency and carrier level.

Feb 17 and 18 PABI #4 (9 mos follow-up). Penetrating electrodes still not eliciting auditory sensations at charge limit (also no non-auditory side effects). Patient is using device all day with surface electrodes and highly satisfied with sound quality. No open-set word identification was measured with ABI alone. Psychophysical testing focused on modulation detection as a function of both loudness of the carrier and of modulation frequency. X-Rays were taken to determine the location and orientation of the penetrating array. Stenver's view X-rays indicate the penetrating array moved since insertion, with electrodes pointing in incorrect direction. A more complete analysis of X-rays will be presented in future progress report.

Mar 1 PABI #5 (about 8 mos follow-up). Penetrating electrodes still not eliciting auditory sensations at charge limit (also no non-auditory side effects). Patient is using device all day with surface electrodes and satisfied with sound quality. No open-set word identification was measured with ABI alone. No psychophysical testing was done on this visit due to the poor condition of patient's general health.

Mar 8 and 9 PABI #2 (about 1 yr follow-up). Modest open-set sentence recognition – no clear improvement over time. Psychophysical testing focused on modulation detection as a function of modulation frequency and carrier loudness, intensity discrimination, and electrode interaction measures.

March 15 and 16 PABI #1 tested (about 18 mos follow-up). Modest improvements have been observed in speech recognition measures over time. No clear changes in thresholds and dynamic ranges on surface or penetrating electrodes. Psychophysical testing focused on modulation detection as a function of both loudness of the carrier and of modulation frequency.

All follow-up data submitted to Cochlear Corporation for IDE submissions.

Other Activities:

Discussions during ABI Team meetings regarding redesign of 2nd generation PABI (larger surface area on PABI electrodes, higher charge limit, adding 2 electrodes to the PABI array, adding radio-opaque symbol to electrode carrier).

Programmer Mark Robert is modifying existing psychophysical testing software and programming new experiments for pitch ranking and comparisons of surface and penetrating electrodes, and for comparing pitch in PABI and acoustic hearing for PABI#3 who has residual hearing in contralateral ear.

Summary:

All PABI recipients are able to use their implants with varying benefit, typical of regular surface ABI recipients. Two patients did not receive hearing on their penetrating electrodes, but all patients' surface electrodes have provided useful auditory sensations. The PABI provides hearing sensations at lower levels of electrical stimulation than the surface ABI, with a range of pitch sensations, and with objective and subjective benefits when used in combination with surface electrodes.

II/ Activities at HMRI

1/ Changes to the penetrating auditory brainstem implant (PABI) array (Co-ordinated with Cochlear LTD, Cochlear Americas, and The House Ear Institute)

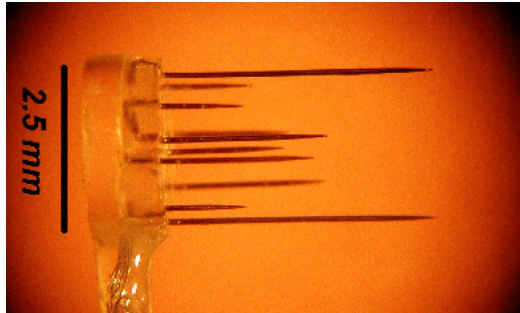


Fig 1

Figure 1 shows the microelectrode array that is fabricated in Sydney, Australia by Cochlear Ltd. It contains 8 discrete activated iridium microelectrodes that range in length from 1-2 mm and also includes two longer (3-mm) electrically inactive anchoring pins which help to stabilize the array within the cochlear nucleus. The iridium microelectrodes are fabricated at HMRI. The physical configuration of the array is according to the specifications set forth by HMRI and HEI, and are based largely on the anatomical studies of Dr. Jean Moore, who remains a consultant to the project.

Based on our results from the first 5 patients who received the penetrating microstimulating array, the Food & Drug Administration has approved extending the study to an additional 10 patients. We have fabricated the microelectrodes for these devices and shipped them to Cochlear LTD In Sydney. Pending approval by the FDA, the new arrays will incorporate two changes from the original design; convert the 2 stabilizing pins to active electrodes and increase the surface area of the microelectrodes to $5,000 \mu\text{m}^2$, from the present $2,000 \mu\text{m}^2$. In conjunction with the latter modification, we have petitioned the FDA to allow us to increase the maximum charge per phase to 8 nC, from the present 3 nC.

Patients who elect to receive the PABI array also receive an array of 14 macro electrodes in their lateral recess.. At present, the penetrating microelectrode array includes 8 active microelectrodes and two longer (3.5 mm) pins of the same diameter, whose function is to mechanically stabilize the array after it has been implanted into the tissue. In the current design, these long pins are electrically inactive. Recent analysis of data from all of the House Ear Clinic's ABI patients by Dr. Robert Shannon shows very high thresholds for auditory percepts elicited by the most medial electrodes on the surface array. This indicates that these electrodes are remote from the cochlear nucleus after the surface array is inserted into the lateral recess. We have concluded that these channels could be used most productively if routed to the stabilizing pins on the penetrating array, which will become active electrodes by removing the Parylene-C insulation from an annular region on their shafts. The area of the each annulus will be $5,000 \pm 500 \mu\text{m}^2$, (21 μm in length on the 75 μm diameter iridium shafts). This removal of the Parylene insulation is easily accomplished with the excimer laser at HMRI, where the electrodes are fabricated.

The annulus on both of the pins will be 2.5 mm below the underside of the array button. In the current design, the microelectrodes range in length from 1 to 2 mm, and the additional electrode sites on the stabilizing pins at 2.5 mm will extend this range, to allow for individual differences in the depth and thickness of the patients' cochlear nucleus and of the overlying glial limitans, and for differences in the placement of the penetrating array. Since the number and lengths of the microelectrodes will be unchanged from the current design, the proposed change will not entail additional risk to the patients. The stabilizing pins will remain 3.5 mm in length, so that the mechanical stability of the penetrating array will not be affected.

In two of our patients with the penetrating auditory brainstem implants (PABIs) the stimulus amplitude has been limited by the charge limit of 3 nC/phase, rather than by the

patients' judgement of maximum comfortable loudness. Therefore, it might be advantageous to raise the charge limits somewhat, provided that this can be done without injury to the neurons and neuropil surrounding the electrodes. We propose to increase the microelectrodes' exposed surface areas, thereby reducing the charge density and current density in the tissue immediately adjacent to the electrode. We investigated this approach in two domestic cats. In the first (CN150), the safety of stimulating at higher charge per phase and lower charge density was investigated. In the second cat (CN151), we investigated how the larger electrode surface area might affect the neuronal activity induced by the microstimulation at levels near the threshold of the auditory percepts in the human patients.

The results from the two animals are summarized below. On the basis of the results from these two cats, We have recommended to the Food & Drug Administration that the surface areas of the microelectrodes used in future penetrating ABIs should be increased to $5,000 \mu\text{m}^2 \pm 500 \mu\text{m}^2$ (from the present $2,000 \mu\text{m}^2$) and that in patients implanted with these devices, the upper limit of charge per phase limits should be increased 8 nC/phase. Since this higher level should induce louder sounds, presumably it would be reached only occasionally with the patient's take-home sound processor. The absolute charge limit of 3 nC/phase for the patients with the PABI arrays of the current design should NOT be increased. In all of the PABI patients, the stimulus pulses rate should be limited to 250 Hz per electrodes, as in the present protocol.

Summary of findings from cat CN150.

We implanted an array of 16 discrete activated iridium electrodes into the ventral cochlear nucleus of an adult cat (CN150). The electrode surface areas were $5,000 \mu\text{m}^2 \pm 500 \mu\text{m}^2$. The electrode shafts were insulated with Parylene-C. Except for the larger active surface areas, the electrodes are identical to those currently in use in the human patients who have received the penetrating Auditory Brainstem Implant.

37 days after implanting the array, the cat was anesthetized with Propofol. We selected 9 electrodes from which we were able to record single or multiple action potentials in response to acoustic stimuli, ensuring that their tips were in the cochlear nucleus. These were pulsed continuously for 8 hours at 250 pulses per second, using charge-balanced, cathodic first pulse pairs (100 μs /phase in duration). The cat was anesthetized during the stimulation, since awake cats apparently perceive continuous stimulation above 4 nC/phase with multiple electrodes in the cochlear nucleus as being uncomfortably loud. 5 channels were pulsed at 8 nC/phase (80 μA) and 4 were pulsed at 6 nC/phase (60 μA). The maximum charge per phase (8 nC) was twice as great at the threshold for tissue damage seen in previous studies in the cat (3-4 nC/phase, McCreery et al, 1994), in which electrodes with surface areas of 500 - $2,000 \mu\text{m}^2$ were used. However, because of the larger surface areas in the present animal, the charge density was only about 40% as great at a particular charge per phase. Also, in the present animal, the stimulus pulse rate was 250 Hz, rather than 500 Hz, as in the earlier study in which the damage threshold was 3-4 nC/phase.

Twenty-three hours after the end of the 8 hours of stimulation, the cat was anesthetized and perfused through the ascending aorta for histologic analysis of the electrode sites. The array was removed from the cochlear nucleus, the nucleus was resected and imbedded into paraffin. 6 μm histologic sections were cut perpendicular to the electrode shafts and stained with Cresyl violet (Nissl stain). Micrographs of thirteen tips sites, including 3 the unpulsed sites that were in the cochlear nucleus, are shown below. Tip sites are marked T.

Histologic evaluation of the electrode sites revealed no differences between the pulsed and unpulsed electrode sites, except for some minimal infiltration of inflammatory cells (probably lymphocytes and macrophages) which are always seen around pulsed microelectrodes. Neurons within 100 μm of the pulsed and unpulsed electrode tip sites

appear normal, and there was no evidence of the vacuolations of the myelinated axons near the pulsed electrodes, which was a cardinal feature of the stimulation-induced injury seen in the earlier animal study (McCreery et al 1994), and which was the basis for the present charge per phase limits for the human patients.

In the earlier study (McCreery et al, 1994) , the occurrence and severity of tissue damage in the ventral cochlear nucleus was correlated strongly with charge per phase, and only weakly with charge density. However, in that study we did not explore the interaction of charge density and charge per phase for the range of charge densities ($160 \mu\text{C}/\text{cm}^2$ and below) used in the present animal. For larger (subdural surface) electrodes, charge density and charge per phase interact synergistically to determine the threshold of tissue injury, and as the charge density decreases, the charge per phase at the damage threshold is greater (McCreery et al, 1990). It is possible that in the present study (cat CN150), the charge density was sufficiently low, and the surface area of the microelectrodes was sufficiently large, such that this synergistic interaction of charge density and charge per phase was beginning to appear. Also, in the present animal, the stimulus pulse rate was 250 Hz, the rate that is used in the ongoing clinical studies. In the earlier study (McCreery et al, 1994), the pulse rate was 500 Hz. The reduced pulsing rate probably contributed significantly to the absence of stimulation-induced damage in cat CN150. In peripheral nerves, the propensity for stimulation-induced axonal damage is strongly and positively correlated with the stimulus pulse rate (McCreery et al 1995).

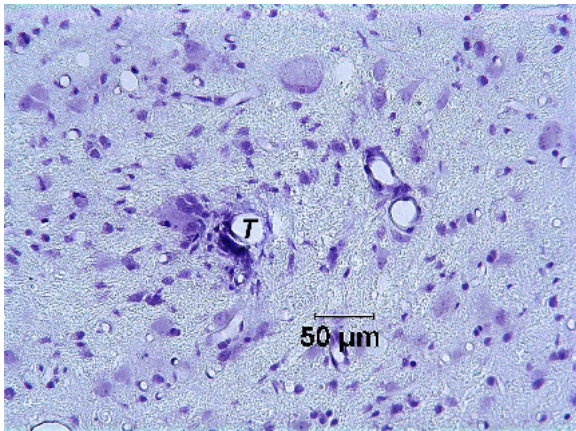
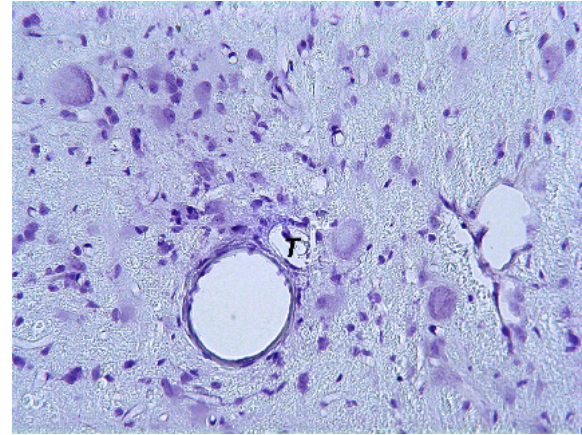
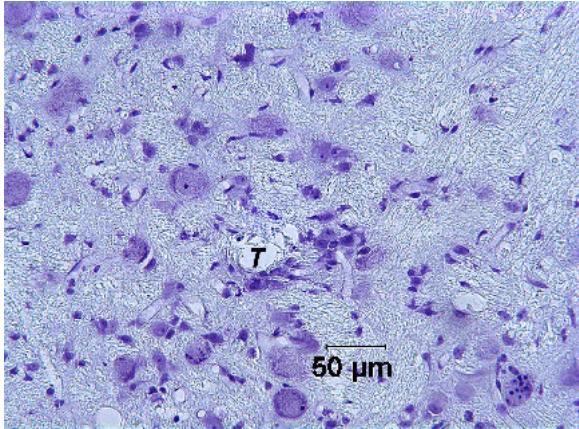


Figure 2: Tip sites of 3 unpulsed electrodes

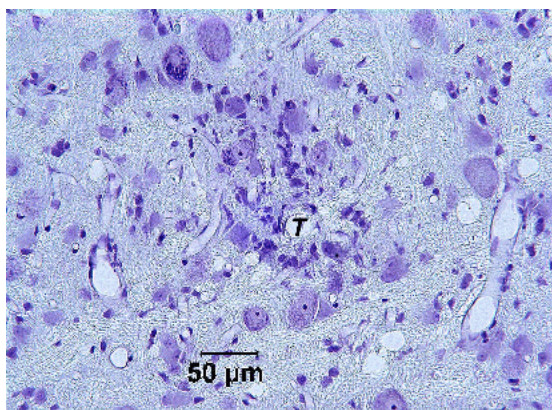
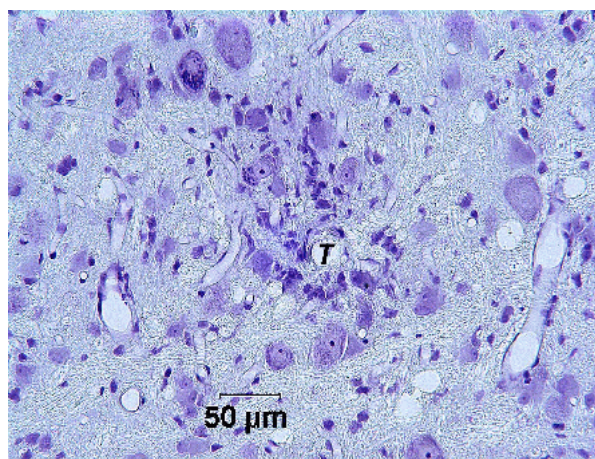
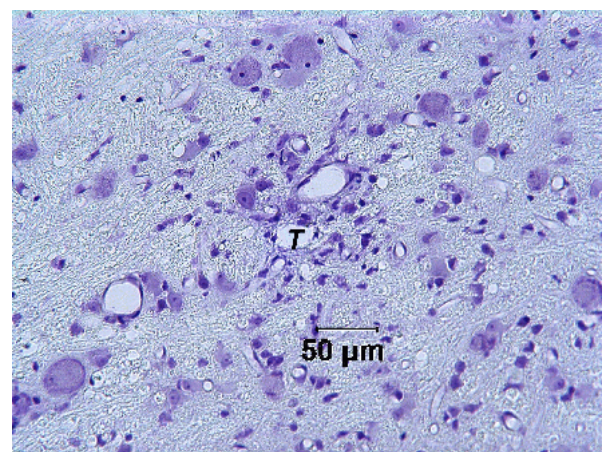
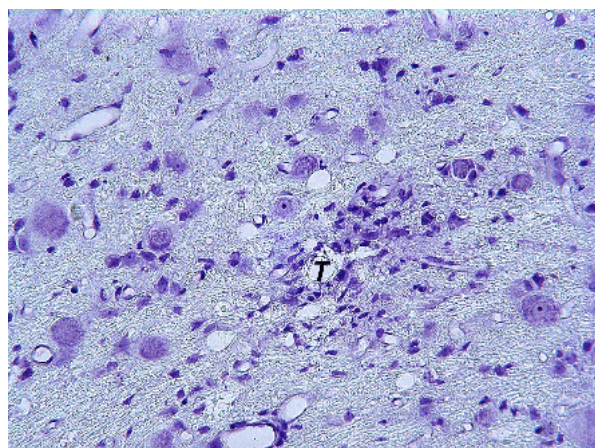
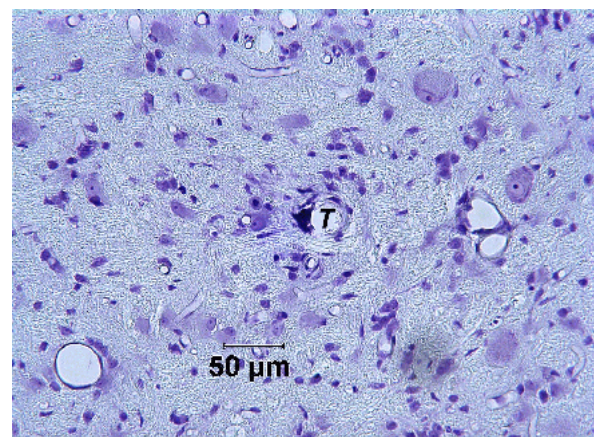


Figure 3: Tip sites of 5 electrodes pulsed at 8 nC/phase

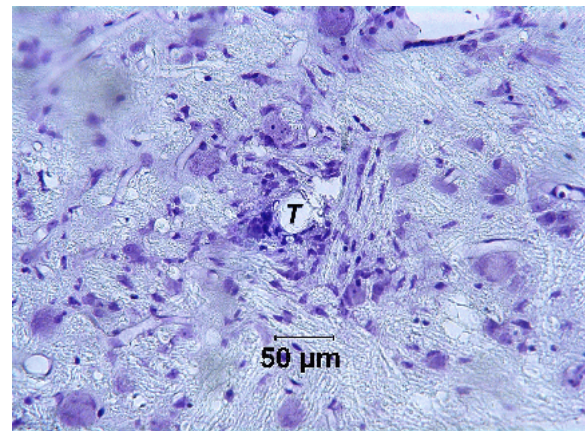
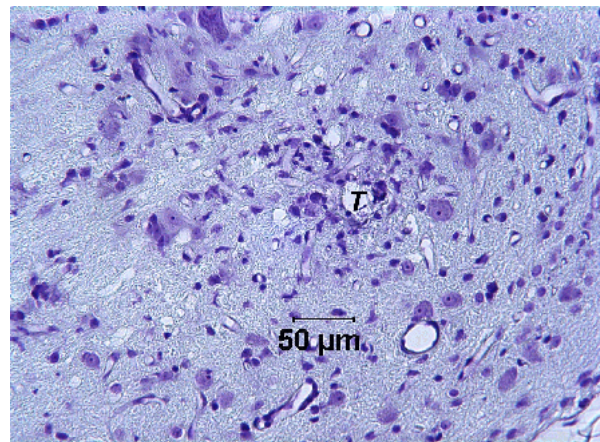
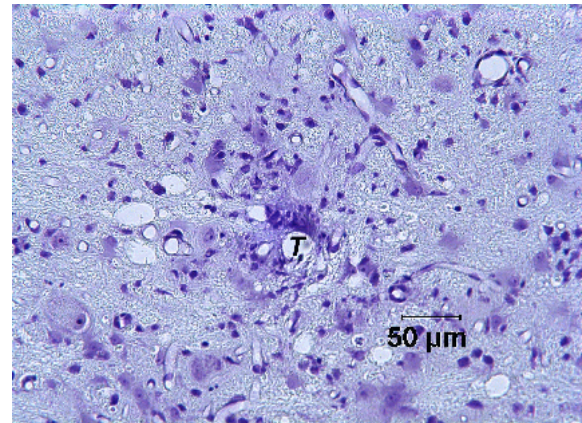
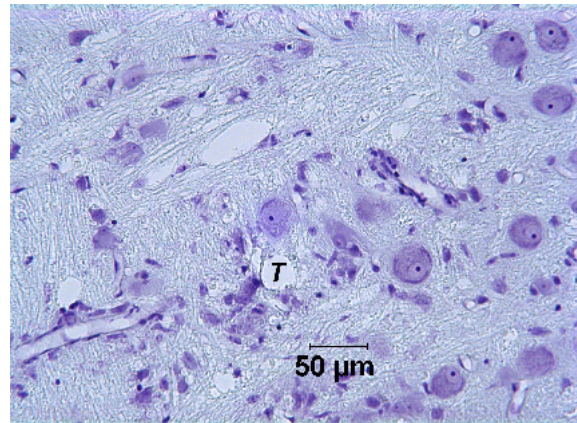
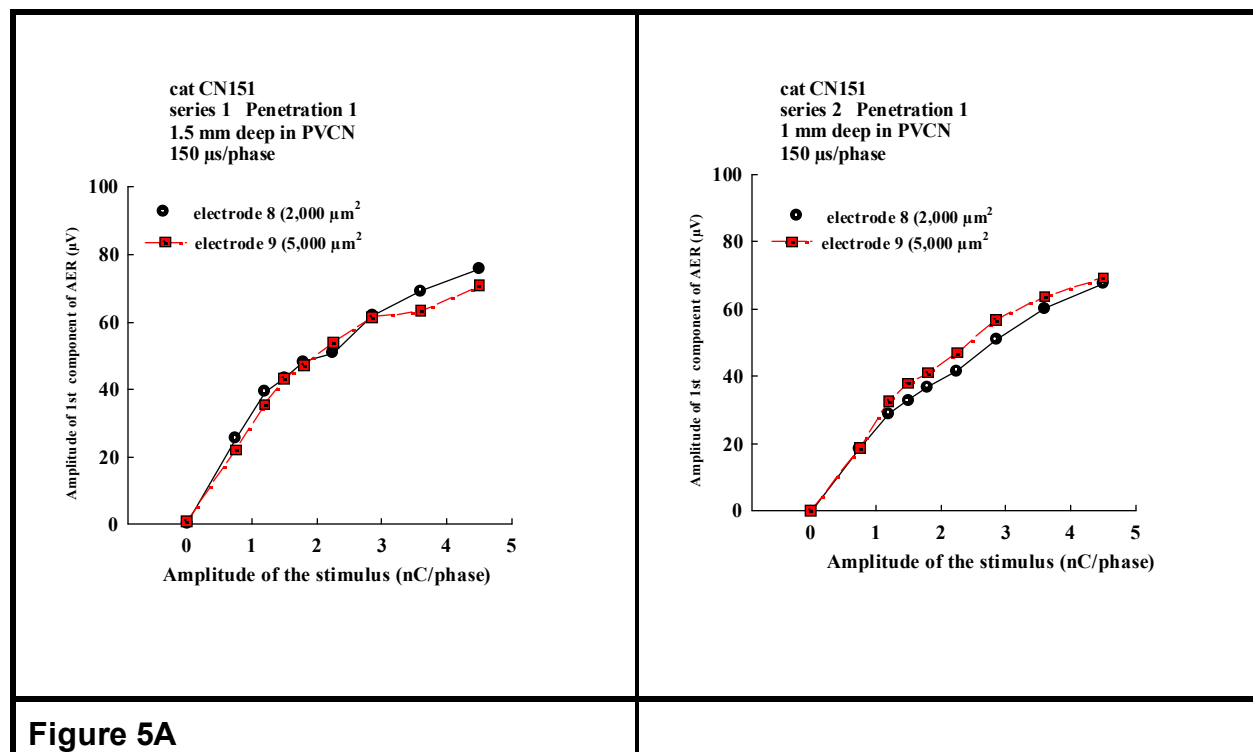


Figure 4: Tip sites of 4 electrodes pulsed at 6 nC/phase

Summary of results from cat CN151

We conducted an acute experiment to determine how the responses evoked in the feline cochlear nucleus by stimulating microelectrodes with surface areas of 2,000 and 5,000 μm^2 differ. The cat was anesthetized with isoflurane and nitrous oxide, and a recording electrode was placed in the right inferior colliculus through a small craniectomy. The left cochlear nucleus was exposed by aspiration of the lateral cerebellum and a pair of activated iridium microelectrodes, one with a surface area of 2,000 μm^2 and one with a surface area of 5,000 μm^2 , and separated by 250 μm , was inserted into the posteroventral cochlear nucleus (PVCN).

The stimulus was controlled-current pulses pairs, at 250 pulses per second. Response growth functions (RGFs) of the amplitude of the earliest component of the compound response evoked by the microelectrodes in the cochlear nucleus, and recorded in the contralateral inferior colliculus, were generated with the pair of microelectrodes at various depths in the PVCN. RGF's were generated for 2 penetrations into the nucleus (Figure 5 and 6, respectively), and with a stimulus pulse duration of 80 or 150 μs /phase. The RGF for the 2,000 and 5,000 μm^2 electrodes are shown in Figures 5 and 6. Each pair of RGFs, one from each electrode, at a particular location in the cochlear nucleus and for a particular stimulus pulse duration, is designated as a "series". At some location, anodic-first and cathodic-first pulse pairs were evaluated. As expected, the RGFs generated by stimulating at different locations in the cochlear nucleus differed, but the RGFs from any particular location are very similar for the 2,000 and 5,000 μm^2 microelectrodes, and there are no consistent differences. In the human patients, the thresholds of the auditory percepts evoked from the penetrating electrodes have been in the range of 0.5 to 1 nC per phase. In this range, in cat CN151 there were no consistent difference in the amplitude of the neuronal responses evoked by the 2,000 and 5,000 μm^2 microelectrodes. This implies that the threshold of the patients' auditory percepts will not be increased significantly if the surface areas of the microelectrodes is increased to 5,000 μm^2 , from the present 2,000 μm^2 .



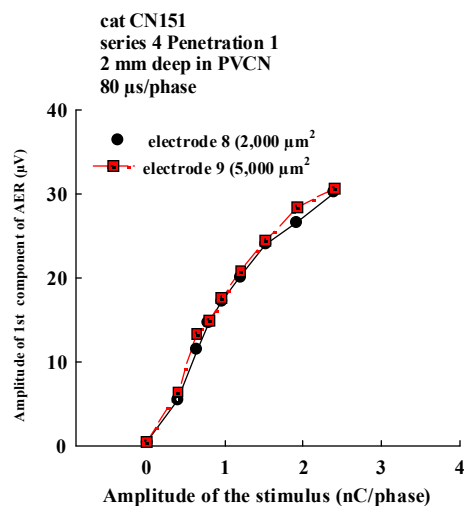
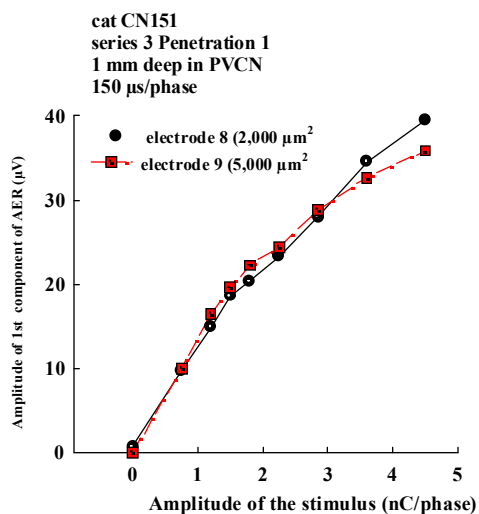


Figure 5B

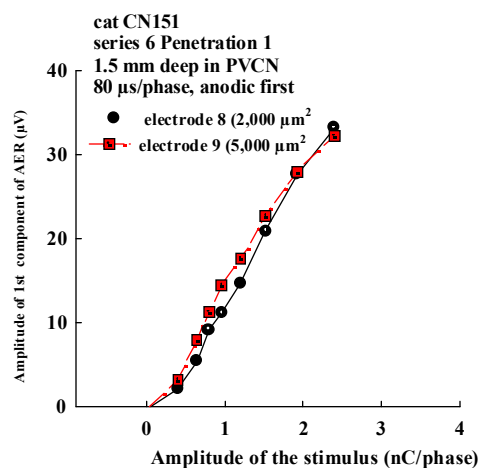
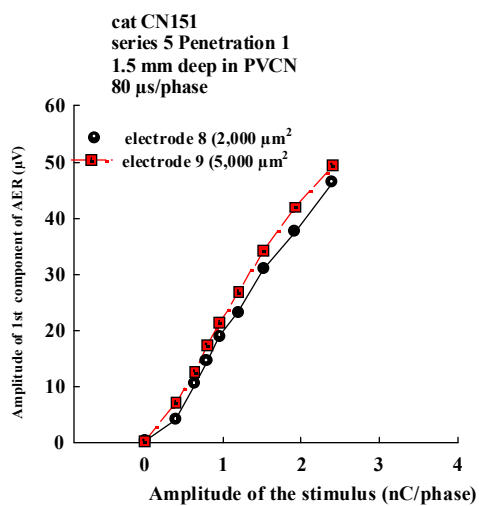


Figure 5C

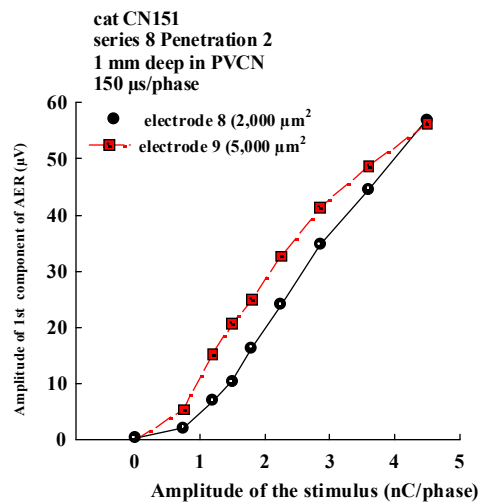
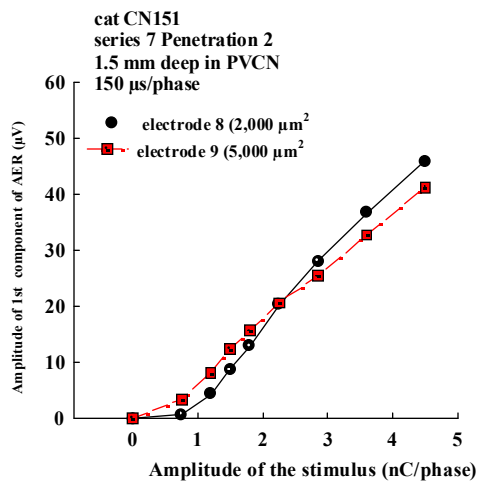


Figure 6

2/ Evaluation of chronically-implanted silicon-substrate microelectrode arrays In the cat cochlear nucleus

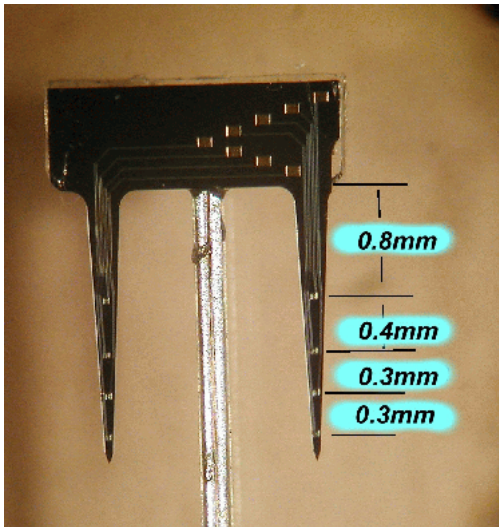


Fig 7A

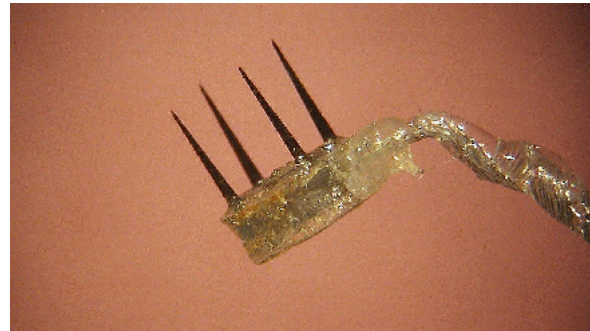


Fig 7B

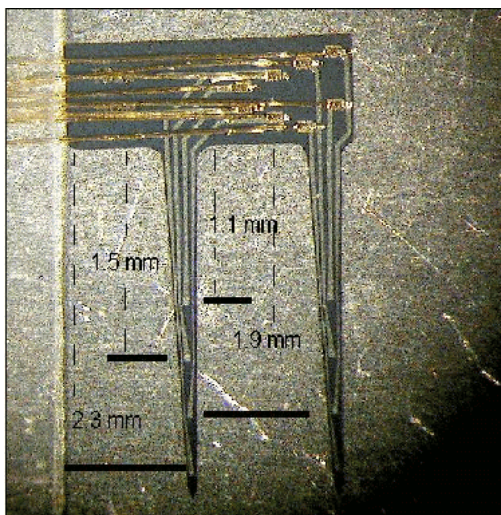


Figure 7C

The workscope of our contract calls for the development of arrays of silicon substrate electrodes, which should allow placement of many more electrode sites into the human cochlear nucleus than is possible with discrete iridium microelectrodes. We are developing arrays for implantation into the human cochlear nucleus that have 16 electrode sites distributed on 4 silicon shanks extending from an epoxy superstructure that is 2.4 mm in diameter. This is the same footprint as our first-generation human arrays employing discrete iridium microelectrodes and is designed to be implanted using the same inserter tool.

We have been conducting animal studies using arrays with silicon substrate probes fabricated at the University of Michigan under the direction of Design Engineer Jamille Hetke. Figure 7A shows a probe with

2 shanks and 8 stimulating sites, that have been sputter-coated with iridium oxide. The 4 sites on each shank are located between 0.8 to 1.7 mm below the top of the shanks. Figure 7B shows an array with 2 of the probes (4 shanks and 16 electrode sites) extending from an epoxy superstructure that floats on the surface of the cochlear nucleus. The cable is angled vertically, to accommodate the trans-cerebellar approach to the feline cochlear nucleus.

Six cats have been implanted with arrays containing the probes depicted in Figure 7A. These animals have been reported in previous quarterly reports. One cat (CN149) remains alive and well at 237 days after the implant surgery. Figure 7C shows a modified probe in which the electrode sites are slightly further from the probes, transverse spine, thus placing the sites deeper in the cats' cochlear nucleus. As described below, this arrangement seems to place most of the electrode sites in the ventral cat's ventral cochlear nucleus when the arrays are implanted from the nucleus's dorsolateral surface.

Using aseptic technique, the cat's scalp is opened in a midline incision, and the muscles reflected. A small craniectomy is made over the right occipital cortex and the bipolar

recording electrode is introduced into the rostral pole of the right inferior colliculus. To access the cochlear nucleus, a craniectomy is made over the left cerebellum, extending up to the tentorium. The rostralateral portion of the left cerebellum is aspirated using glass pipettes. The electrode array is secured on the end of a vacuum wand, and thereby advanced into the cochlear nucleus.

The array cable is fixed to the edge of the craniectomy with cyanoacrylate cement and the introducer is withdrawn. The surgical site is filled with gelfoam and the craniectomy is closed with methacrylate bone cement.

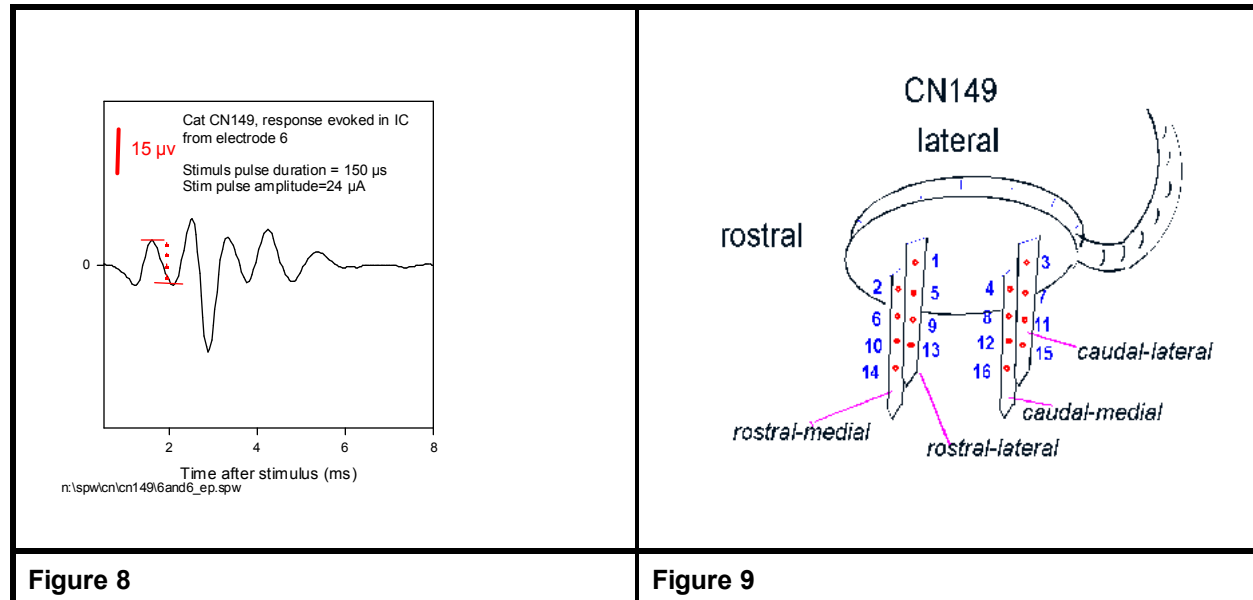


Figure 8 shows an averaged evoked response (AER) recorded in the right inferior colliculus (IC) in response to electrical stimulation in the cochlear nucleus with microelectrode #6 of cat CN149. 1024 successive responses were averaged to obtain this AER. Response growth functions (RGFs) were generated from the amplitude of the earliest component of the AERs, measured from the peak of the first positivity to the subsequent negativity as shown in the figure. Figure 9 shows the positions of the 16 electrode sites on the shanks of the array in cat CN149. Low-numbered sites are close to the array superstructure and, thus are more dorsal and lateral in the nucleus when the electrode is inserted from the dorsolateral surface of the CN. Array CN149 contained probes of the type depicted in Figure 7A.

Figure 10A-P show the RGFs from the IC of cat CN-149 as evoked from each of the 16 microelectrode sites in the CN, at 14, 43, 195 and 237 days after implantation of the array into the CN. The thresholds of the RGFs evoked from electrode sites 1-4 increase markedly between the 14th and 237th day, and the slope of the RGFs decreased, with most of the change occurring between days 14 and 43. These changes may be due to the electrode sites being displaced slightly toward the dorsal boundary of the ventral cochlear nucleus by the growth of connective tissue under the array matrix. The RGFs evoked from the deeper sites were more stable with little change between days 43 and 237. Curiously, the responses recorded on day 195 were slightly depressed on most channels.

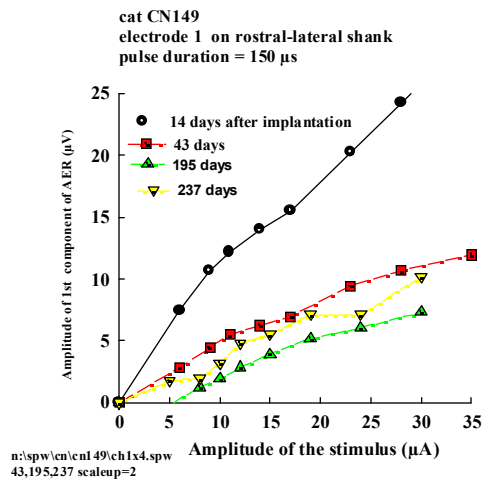


Figure 10A

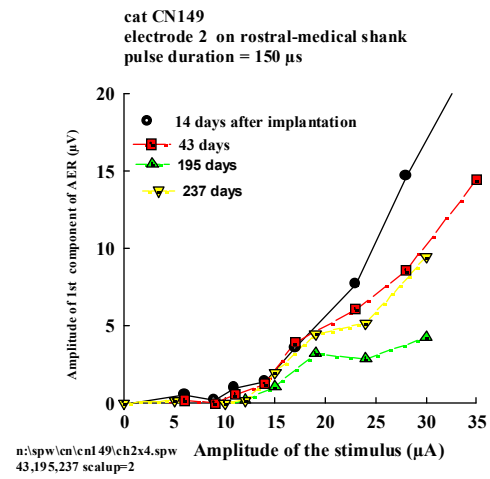


Figure 10B

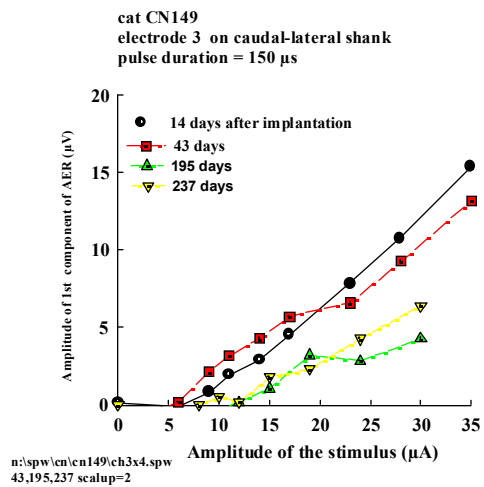


Figure 10C

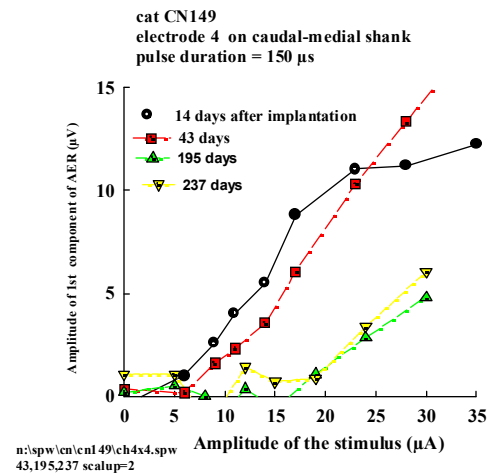


Figure 10D

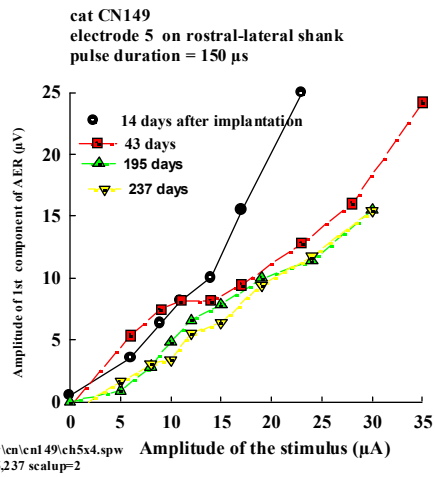


Figure 10E

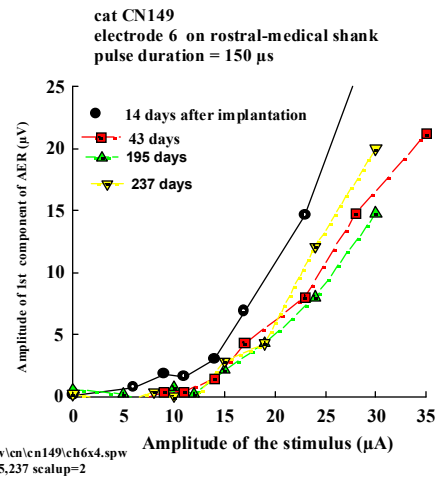


Figure 10F

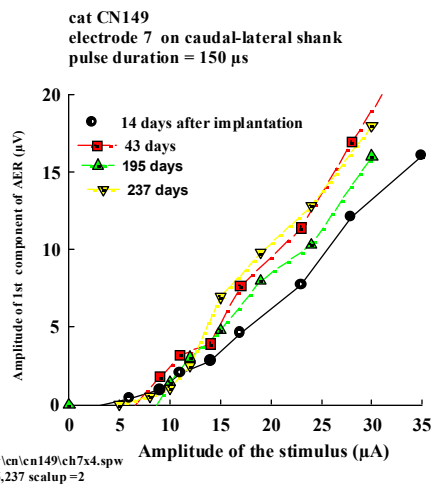


Figure 10G

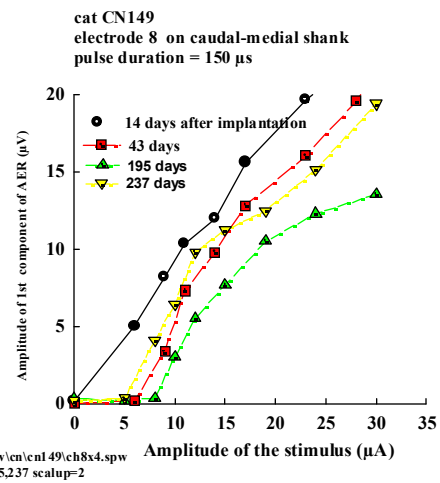


Figure 10H

cat CN149
electrode 9 on rostral-lateral shank
pulse duration = 150 μ s

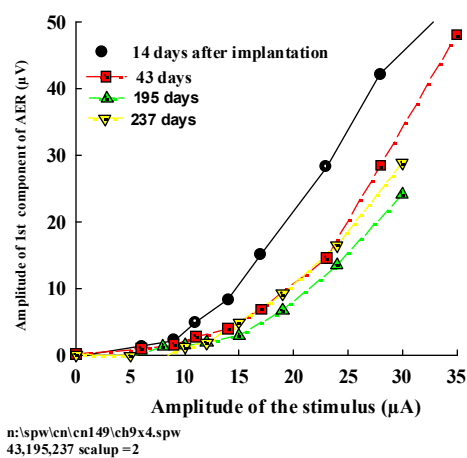


Figure 10I

cat CN149
electrode 10 on rostral-medial shank
pulse duration = 150 μ s

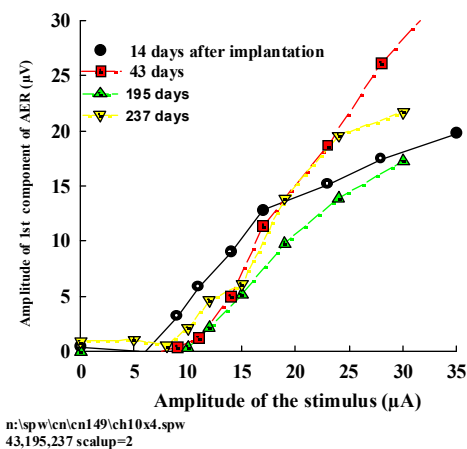


Figure 10J

cat CN149
electrode 11 on caudal-lateral shank
pulse duration = 150 μ s

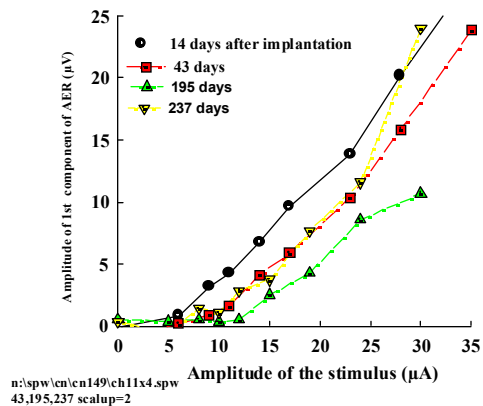


Figure 10K

cat CN149
electrode 12 on caudal-medial shank
pulse duration = 150 μ s

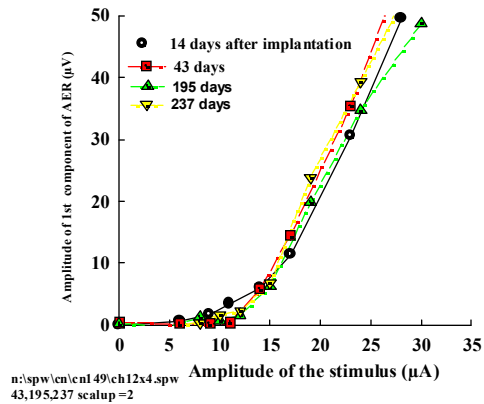


Figure 10L

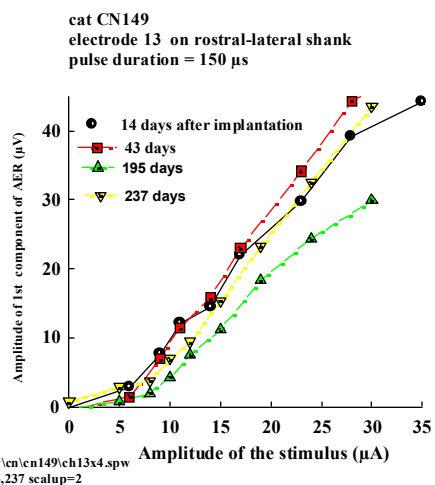


Figure 10M

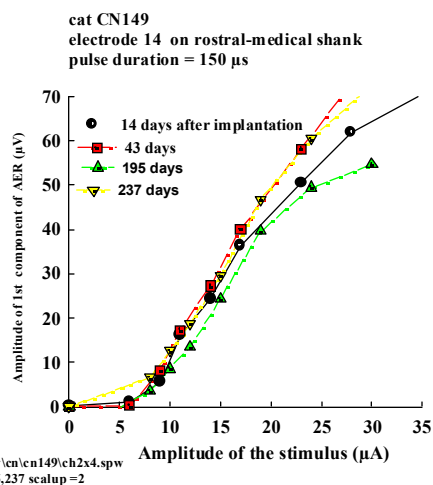


Figure 10N

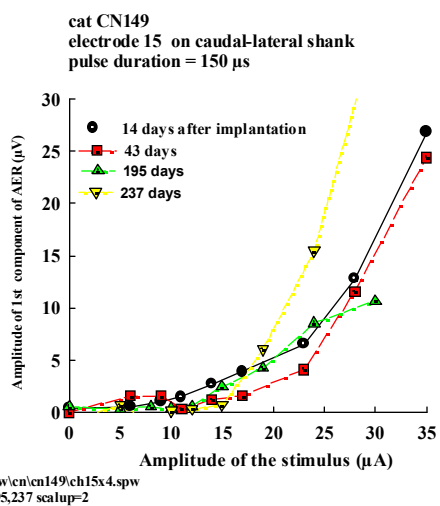


Figure 10O

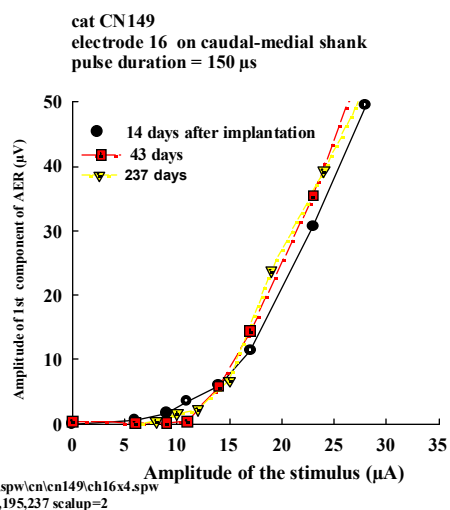
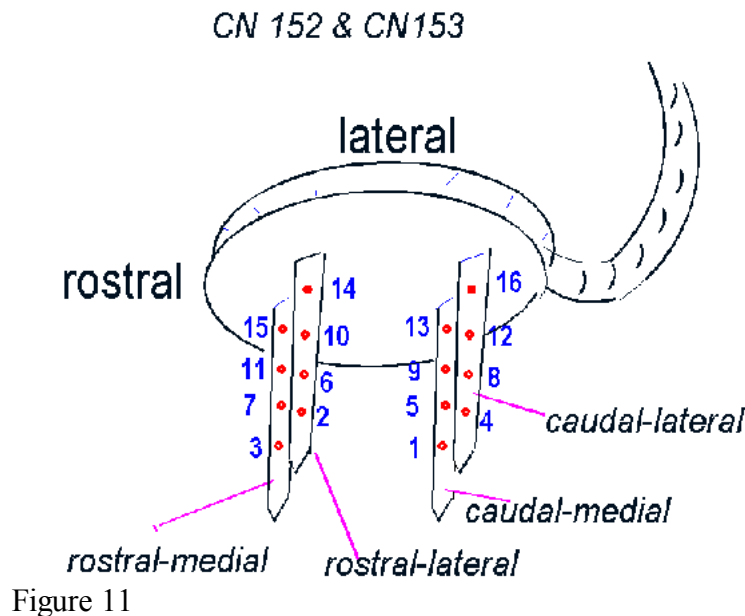


Figure 10P

Figure 11 shows the distribution of the sites on the arrays implanted in cats CN152 and 153, who received their implants during the past quarter. These arrays contain probes of the type depicted in Figure 7C, in which the sites are slightly farther from the array's superstructure and, thus slightly more ventral and medial in the cochlear nucleus. Note that in these arrays, the low-numbered sites are deepest in the CN. Figure 12A-D shows the RGFs from the 4 sites on each of the 4 shanks from cat CN152 at 45 days after implantation. On the caudal-medial and caudal-lateral shanks, the deepest sites evoke only weak responses, and thus, these probably are outside of (ventromedial to) the ventral cochlear nucleus. Conversely, on the rostral-medial shank, the shallowest site appears to be dorsal to the ventral cochlear nucleus. On the rostral-lateral shank, the threshold of the response evoked from the shallowest site (#14) also is high.

Figure 13 shows the RGFs from cat CN153 at 22 days after implantation. In this cat, the thresholds of the RGFs from the shallowest sides on the caudal-lateral and caudal-medial shanks are high, suggesting that they are on the dorsal margin of the posteroventral cochlear nucleus. This is in contrast to the situation in cat CN152 in which the deepest sites on the caudal shanks appear to have been slightly deep to the nucleus. On the rostral-lateral and posteromedial sites, the threshold of all of the RGFs is 5 μ A or less, indicating that all sites are in the ventral nucleus. These data suggest that distribution of sites on the new probe (Figure 7C) can span all or most of the feline ventral cochlear nucleus when the array is inserted from the nucleus' dorsolateral surface.



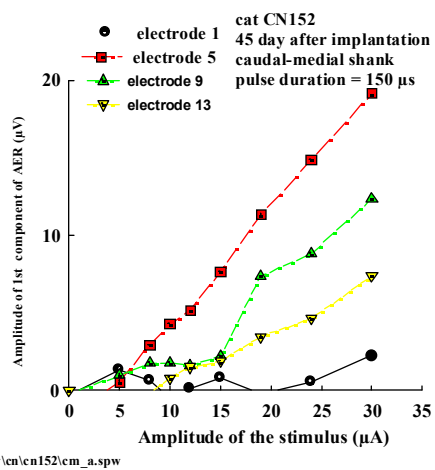


Figure 12A

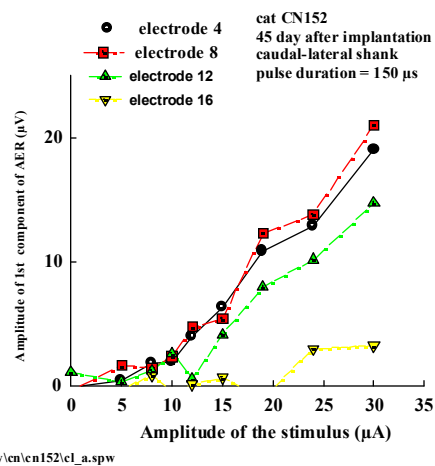


Figure 12B

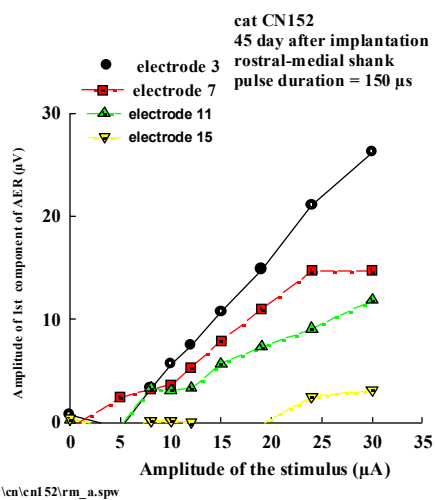


Figure 12C

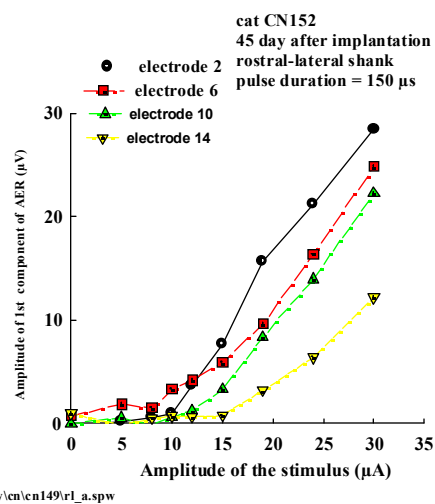


Figure 12D

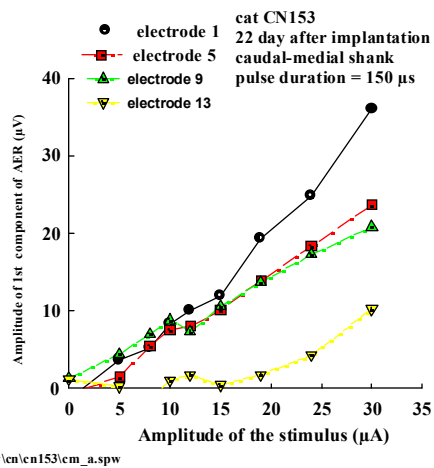


Figure 13A

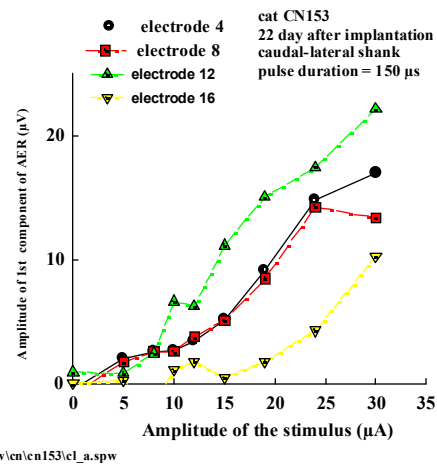


Figure 13B

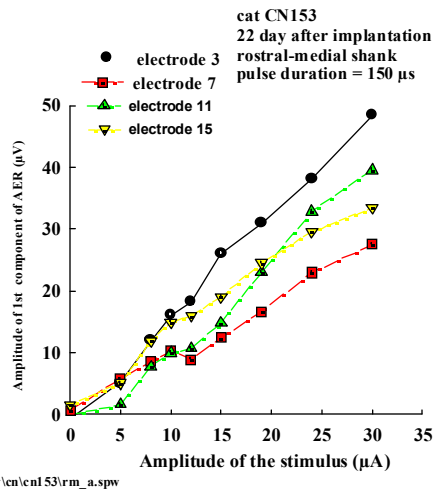


Figure 13C

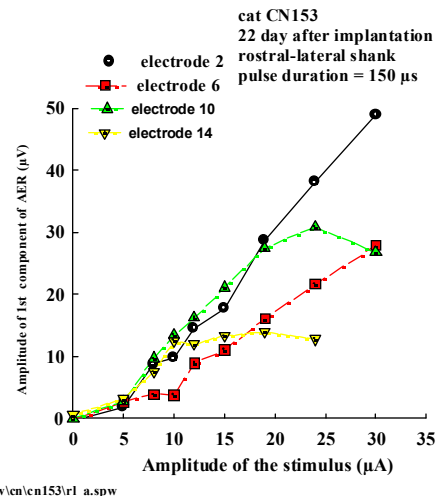


Figure 13D

3/ Preparations for multisite microstimulation in the cat cochlear nucleus with multisite recording in the inferior colliculus.

Cat CN149, 152, 153 and all subsequent animals with chronic cochlear nucleus implants will undergo terminal experiments in which evoked potentials and single units will be recorded from 16 sites in the central nucleus of the inferior colliculus during stimulation with the 16 microelectrode sites in the cochlear nucleus. These studies will afford a good survey of the ability of the different microelectrode sites in the ventral cochlear nucleus to activate different neuronal populations in the ventral CN over a range of stimulus amplitudes. In preparation for these studies, a double-walled sound chamber has been installed in our laboratory at HMRI. This has been equipped with a surgery table, a floor-standing binocular microscope, ultra low nose anesthesia apparatus for delivering an oxygen- isoflurane mixture to the cat, and a circulating water heating pad. We have installed equipment to monitor the animal's electrocardiogram, expired CO₂, respiration rate and temperature. Hardware and computer software for 16-channel stimulating and recording has been completed. Thirty-two-channel silicon substrate probes have been ordered from NeuroNexus, Inc., and are scheduled to be delivered in June. At first, these will

be used in terminal acute studies of the cats with the chronic implants in the CN, but we also plan to adapt the probes to our chronically implantable deep brain array, so that the same studies can be conducted serially, and with the cats unanesthetized.

Discrimination (detection) and sorting of extracellularly-recorded unit action potentials (spikes)

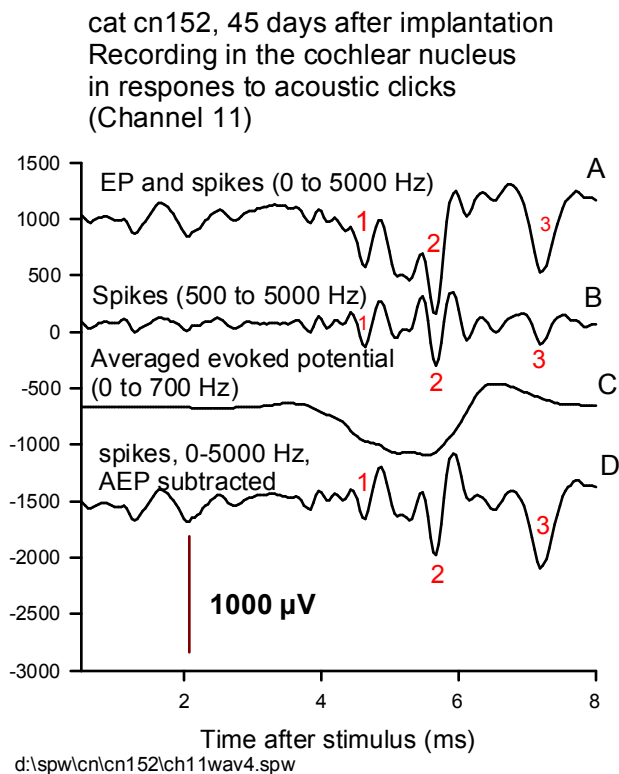


Figure 14

with $\text{Cos}(t)/t$ weighting and with a half-power passband of 500-5000 Hz. The evoked potential has been effectively eliminated from the trace, and the waveforms and amplitudes of spikes 1 and 2 are relatively unaffected. However, spike 3 was of long duration and its frequency spectrum overlaps with that of the evoked potential. Consequently, the high-pass filtering caused significant attenuation of its amplitude.

We have been investigating alternative methods of separating the spikes and the evoked potential that do not suffer from this limitation. One approach is applicable when the time of occurrence of the spikes is somewhat variable relative to the stimulus, (or when their time occurrence is very stable but there is a low probability of their occurrence in each presentation of the stimulus), and if the latency of the evoked potential is very stable relative to the stimulus, and the evoked potential is of nearly constant amplitude after each presentation of the stimulus. Trace C shows the averaged evoked response generated by averaging 5,000 successive occurrences of the acoustic stimulus. Trace D shows the result of subtracting this template from the unfiltered recording, trace A. The evoked potential has been eliminated from the baseline, allowing detection and sorting of the spikes, whose amplitude and shape have not been altered by band pass filtering.

We have incorporated into our spike analysis software the ability to separate the spikes and the evoked potentials either by bandpass filtering with a time-domain filter or by subtracting the averaged evoked potential.

4/ Fabrication of silicon substrate multisite probes at HMRI.

The silicon probes fabricated for us at the CNCT at the University of Michigan have been invaluable in our development of multisite arrays for chronic stimulation in the cochlear nucleus. However, these probes are fabricated using the boron etch-stop method, and as such, they are very thin (15 μ m). The thin silicon substrates are further stressed by the boron doping. These factors render the probes quite fragile, and we expect that this will significantly complicate the process of eventually certifying the arrays for human use. We are developing a process for fabricating silicon probes by deep reactive ion etching. These will be 90-100 μ m in thickness. We have contracted with the California Institute of Technology for access to the semiconductor fabrication clean room of the Micromachining

recorded in the inferior colliculus in response to pulsatile electrical stimulation is complicated by the spikes being superimposed upon a large evoked potential. Carefully matched bandpass filtering to separate the spikes and evoked potential is possible, but the frequency spectra of the spikes overlaps somewhat with that of the evoked potential, particularly for spikes of relatively long duration, and thus the amplitude and waveform of the spike may be distorted by the filtering. This complicates subsequent spike sorting. This problem is illustrated in Figure 14. These data were recorded from electrode 11 on the caudal-medial shank of the microelectrode array in the ventral CN of cat CN152, 45 days after implantation of the microelectrode array in this cochlear nucleus. The response in the cochlear nucleus was evoked at each of the 16 electrode sites in response to brief (150 μ s) acoustic clicks, approximately 55 db msp, which occur at $t=0$ (the left edge of the graph's abscissa). The upper trace (A) shows the unfiltered response (passband of 0-5000 Hz). Three spikes (1,2,3) are superimposed on the evoked potential. The trace B shows the results of high-pass filtering. This was done with a pair of time domain (convolution) filters

Laboratory. One of our staff scientists (M.H.) is spending 50% of his time at this facility. We expected to have our first probes in approximately 3 months.

References cited

McCreery, D. B., T. G. Yuen, W. F. Agnew and L. A. Bullara (1994). "Stimulus parameters affecting tissue injury during microstimulation in the cochlear nucleus of the cat." Hear Res 77(1-2): 105-15.

McCreery, D. B., W. F. Agnew, T. G. Yuen and L. Bullara (1990). "Charge density and charge per phase as cofactors in neural injury induced by electrical stimulation." IEEE Trans Biomed Eng 37(10): 996-1001.

McCreery, D. B., W. F. Agnew, T. G. Yuen and L. A. Bullara (1995). "Relationship between stimulus amplitude, stimulus frequency and neural damage during electrical stimulation of sciatic nerve of cat." Med Biol Eng Comput 33: 426-9.